HHS Public Access

Author manuscript

Biol Psychiatry. Author manuscript; available in PMC 2022 August 08.

Published in final edited form as:

Biol Psychiatry. 2021 March 01; 89(5): 497–509. doi:10.1016/j.biopsych.2020.06.021.

Network Effects of the 15q13.3 Microdeletion on the Transcriptome and Epigenome in Human-Induced Neurons

Siming Zhang[1], **Xianglong Zhang**[2], **Carolin Purmann**[2], **Shining Ma**[3], **Anima Shrestha**[4], **Kasey N Davis**[2], **Marcus Ho**[2], **Yiling Huang**[2], **Reenal Pattni**[2], **Wing Hung Wong**[3], **Jonathan A Bernstein**[5], **Joachim Hallmayer**[2], **Alexander E Urban**[6]

[1]Department of Genetics, School of Humanities and Science, Stanford University, Stanford, California.

[2]Department of Psychiatry and Behavioral Sciences, School of Humanities and Science, Stanford University, Stanford, California.

[3]Department of Pediatrics, School of Humanities and Sciences, Stanford University, Stanford, California.

[4]School of Medicine, Stanford University, and Department of Statistics, School of Humanities and Sciences, Stanford University, Stanford, California.

[5]Department of Human Biology, School of Humanities and Science, Stanford University, Stanford, California.

[6]Department of Genetics, School of Humanities and Science, Stanford University, Stanford, California; Department of Psychiatry and Behavioral Sciences, School of Humanities and Science, Stanford University, Stanford, California.

Abstract

BACKGROUND: The 15q13.3 microdeletion is associated with several neuropsychiatric disorders, including autism and schizophrenia. Previous association and functional studies have investigated the potential role of several genes within the deletion in neuronal dysfunction, but the molecular effects of the deletion as a whole remain largely unknown.

METHODS: Induced pluripotent stem cells, from 3 patients with the 15q13.3 microdeletion and 3 control subjects, were generated and converted into induced neurons. We analyzed the effects of the 15q13.3 microdeletion on genome-wide gene expression, DNA methylation, chromatin accessibility, and sensitivity to cisplatin-induced DNA damage. Furthermore, we measured gene expression changes in induced neurons with CRISPR (clustered regularly interspaced short palindromic repeats) knockouts of individual 15q13.3 microdeletion genes.

RESULTS: In both induced pluripotent stem cells and induced neurons, gene copy number change within the 15q13.3 microdeletion was accompanied by significantly decreased gene expression and no compensatory changes in DNA methylation or chromatin accessibility,

Address correspondence to Alexander E. Urban, Ph.D., at aeurban@stanford.edu.

The authors report no biomedical financial interests or potential conflicts of interest.

Supplementary material cited in this article is available online at https://doi.org/10.1016/j.biopsych.2020.06.021.

supporting the model that haploinsufficiency of genes within the deleted region drives the disorder. Furthermore, we observed global effects of the microdeletion on the transcriptome and epigenome, with disruptions in several neuropsychiatric disorder–associated pathways and gene families, including Wnt signaling, ribosome function, DNA binding, and clustered protocadherins. Individual gene knockouts mirrored many of the observed changes in an overlapping fashion between knockouts.

CONCLUSIONS: Our multiomics analysis of the 15q13.3 microdeletion revealed downstream effects in pathways previously associated with neuropsychiatric disorders and indications of interactions between genes within the deletion. This molecular systems analysis can be applied to other chromosomal aberrations to further our etiological understanding of neuropsychiatric disorders.

Keywords

15q13.3; Copy number variants; CRISPR–Cas9; Genomics; Induced pluripotent stem cells; Neurons

---

The 15q13.3 microdeletion (OMIM 612001) is a 1.5- to 2.0- Mbp deletion on chromosome 15 (1). This copy number variant (CNV) was first reported in 2008 in 9 individuals with intellectual disability, seizures, and mild facial dysmorphism (2). Since then, many other phenotypes have been associated with the CNV, including autism spectrum disorder (ASD), schizophrenia, attention-deficit/hyperactivity disorder, and hypotonia (1,3,4). The most common form of the 15q13.3 microdeletion results in the loss of 8 genes: *CHRNA7, FAN1, TRPM1, KLF13, OTUD7A, MTMR10, ARHGAP11B, and MIR211* (3). Based on association studies and functional neuronal studies, several of these genes, including CHRNA7 (5–8), *OTUD7A* (9,10), *FAN1* (11,12), and *ARHGAP11B* (13), have been suggested as candidates for playing a role in the associated clinical phenotypes. However, little is known about which downstream molecular mechanisms are affected by individual candidate genes or by the CNV as a whole. To date, only one study has characterized the transcriptome-wide effects of the CNV in human tissue, using non-neuronal (lymphoblastoid) cells (14). Current knowledge is even more limited concerning any associated changes in epigenetic processes, which are dysregulated in a number of neuropsychiatric disorders associated with this CNV (15).

In the current study, we analyzed the changes in gene expression, DNA methylation, and chromatin accessibility in induced pluripotent stem cells (iPSCs) with heterozygous 15q13.3 microdeletions as well as in iPSC-derived early-stage induced neurons (iNs) that can mature to resemble excitatory projection neurons. We observed genome-wide changes in all three analyses affecting genes and pathways linked to neuronal dysfunction, including Wnt signaling, cell adhesion, DNA binding and repair, and protein synthesis. Many of these pathways were also found to be disrupted in our gene expression analysis of isogenic cell lines with individual knockouts of 15q13.3 microdeletion genes, where different gene knockouts sometimes converged on similar pathways, indicating synergistic interactions between genes within the CNV.

METHODS AND MATERIALS

Cell Line Characterization

Fibroblasts from 3 patients with heterozygous 15q13.3 microdeletions and neurocognitive symptoms and 3 control subjects (Figure 1A and Table S1 in Supplement 2) were reprogrammed into iPSCs and differentiated into iNs using the neurogenin-2 induction method (16), with downstream analysis at day 6 (Figure 1B). Cell type identity was verified with immunohistochemical staining. See Supplement 1 for details.

CRISPR/Cas9 Knockout of 15q13.3 Microdeletion Genes

Homozygous knockouts of single 15q13.3 microdeletion genes were generated in 4 control iPSC lines using CRISPR/ Cas9 (clustered regularly interspaced short palindromic repeats/ Cas9) (Tables S2 and S3 in Supplement 2). Clonal lines were isolated with limiting dilution and confirmed with Sanger sequencing. See Supplement 1 for details.

Whole-Genome DNA Sequencing

DNA sequencing libraries were generated with the TruSeq DNA Nano Library Kit (Illumina, San Diego, CA) and sequenced on the Illumina HiSeq X. DNA sequencing analysis was carried out using BWA (17), BEDtools (18), and CNVnator (19). See Supplement 1 for details.

RNA Sequencing

RNA sequencing (RNA-Seq) libraries were prepared using the NEBNext Ultra Directional RNA Library Prep Kit (New England Biolabs, Ipswich, MA) and sequenced on the Illumina NextSeq 500 and HiSeq X. RNA-Seq analysis was carried out using Tophat (20), DESeq2 (21), WebGestalt (22), and Ingenuity Pathway Analysis (Qiagen, Hilden, Germany). See Supplement 1 for details.

Genome-wide Targeted Capture DNA Methylation Sequencing

DNA methylation sequencing (Methyl-Seq) libraries were prepared using the SeqCap Epi System (Roche, Basel, Switzerland) and sequenced on the Illumina HiSeq 4000. Methyl-Seq analysis was carried out using Bowtie 2 (23), Bismark (24), MethylKit (25), Metilene (26), and WebGestalt (22). See Supplement 1 for details.

Assay for Transposase-Accessible Chromatin Sequencing

Assay for transposase-accessible chromatin sequencing (ATAC-Seq) libraries were generated as previously described (27) and sequenced on the Illumina NextSeq 500. ATAC-Seq analysis was performed using Bowtie 2 (23), MACS2 (28), and DiffBind (29). Homer motif enrichment analysis (30) was performed as previously described (31). See Supplement 1 for details.

Correlation Analysis

We calculated the Pearson correlations between gene expression, DNA methylation, and chromatin accessibility using genes that were significant (adjusted p value [p_{adj}] ≤ .05)

in at least one of the datasets within each pairwise comparison. For the Methyl-Seq and ATAC-Seq analyses, only genes with significant differentially methylated regions (DMRs) or peaks in the promoter (transcriptional start site to 2 kb upstream) were included.

Cisplatin Cell Survival Assay

Day 6 iNs were treated with 0.5 μM cisplatin or saline for 2 hours. After incubation in cisplatin-free medium for 48 hours, surviving iNs were counted using trypan blue staining and normalized to the cell number in a saline control well to give the survival percentage. Statistical significance was calculated using a nested *t* test with GraphPad Prism (San Diego, CA).

RESULTS

Cell Line Characterization

To study the molecular effects of the 15q13.3 microdeletion, we obtained fibroblasts from 3 patients with the 15q13.3 microdeletion and 3 sex-matched control subjects (Table S1 in Supplement 2). Heterozygous 15q13.3 microdeletions in all 3 patient fibroblasts were located between breakpoints 3 and 4 (Figure 1C), which is the most common combination of breakpoints for the 15q13.3 microdeletion (3). iPSCs generated from fibroblasts using Sendai viral reprogramming stained positive for the pluripotency markers SSEA4, TRA-1–60, and Nanog (Figure 1D). iNs generated from iPSCs exhibited neurite morphology and stained positive for the neuronal markers TUJ1, VGLUT1, and MAP2 (Figure 1E). Gene set enrichment analysis (GSEA) showed that genes involved in neuronal processes were upregulated in iNs compared with iPSCs (Figure 1F). As quality control, cell lines were assessed for sample identity, nonparental CNVs, residual Sendai virus expression, cell type composition, and contributors of expression variance (Tables S1, S4, and S5 in Supplement 2 and Figure S1 in Supplement 1). See Supplement 1 for details.

Transcriptional Impact of the 15q13.3 Microdeletion

We performed RNA-Seq on 6 15q13.3 microdeletion clonal lines and 6 control clonal lines to determine the effects of the heterozygous 15q13.3 microdeletion on gene expression (Table S1 in Supplement 2). We first looked for evidence of haploinsufficiency or dosage compensation within the microdeletion. In both iPSCs and iNs, *KLF13, MTMR10, OTUD7A, FAN1,* and *ARHGAP11B* showed significantly decreased expression in 15q13.3 microdeletion cases ($p_{adj} \leq .05$). *CHRNA7* was expressed at very low levels and was nonsignificantly decreased in iPSCs but was significantly decreased in iNs. The final protein-coding gene within the deletion, TRPM1, was not expressed above threshold levels in iPSCs or iNs, which agrees with previous evidence suggesting that it is primarily expressed in the retina (32) (Figure 2A, B).

Although the 15q13.3 microdeletion had a strong impact on genome-wide gene expression, it was not the primary source of variability in the principal component analysis (PCA) (Figure S2A, D in Supplement 1). Genome-wide, 178 genes were differentially expressed (DE) in iPSCs and 369 genes were DE in iNs (Figure 2C, D and Tables S6 and S7 in Supplement 2). The larger number of DE genes in iNs suggests that this CNV may have

stronger downstream effects in a more relevant cell type. At the iN stage, a number of genes were identified as DE that have been previously implicated in neuropsychiatric disorders, including VIPR2 for schizophrenia (33,34); *CACNG3, SCN8A, SPATA5*, and *KCNA2* for epilepsy (35–38); *LINS1* and *DCPS* for intellectual disability (39–41); and *PRODH* and *DGCR6* for both schizophrenia and autism (42,43).

After performing GSEA, we identified no enriched Gene Ontology (GO) molecular function (GOMF) or GO biological process (GOBP) terms in iPSCs. In the iNs, we identified 7 significant GOMF terms and 46 significant GOBP terms, many of which fell under the categories of ribosome function, DNA replication/damage, and Wnt binding (Figure 2E). We performed overrepresentation analysis using Ingenuity Pathway Analysis and within iNs identified an enrichment of the EIF2 signaling pathway ($p_{adj} \leq .05$), which is involved in translational control (44). The genes driving this enrichment included AGO2, which plays a key role in RNA interference; *EIF2AK2*, a kinase that phosphorylates translation initiation factor EIF2S1; and 12 ribosomal protein genes (Figure 2F).

DNA Methylation Analysis

We performed Methyl-Seq on the same cohort of cell lines used for RNA-Seq analysis. One iN control line was excluded from final analysis owing to clustering with iPSCs (Table S1 in Supplement 2). We found no DMRs located in the promoters or gene bodies of the 7 protein-coding 15q13.3 microdeletion genes, which was consistent with the lack of dosage compensation seen in the RNA-Seq data. PCA showed minor separation between deletion cases and controls along PC1 in both cell types (Figure S2B, E in Supplement 1). Genome-wide, 416 DMRs were identified in iPSCs and were annotated to 147 promoter regions, 404 gene bodies, and 77 intergenic regions (Figure 3A, C and Table S8 in Supplement 2). In the iNs, 408 DMRs were identified and annotated to 160 promoter regions, 277 gene bodies, and 80 intergenic regions (Figure 3B, D and Table S9 in Supplement 2).

After assigning DMRs to genes, we performed GSEA on the Methyl-Seq dataset. Both iPSCs and iNs showed an enrichment in cell adhesion and Wnt signaling–related pathways (Figure 3E, F), which were driven mainly by a large number of DMRs located near protocadherins (Figure 3G–I). Protocadherins are cell adhesion proteins that have been implicated in several neurodevelopmental disorders, including epilepsy, ASD, schizophrenia, and Down syndrome (45–47). Besides the protocadherin-related pathways, we also observed an enrichment in 2 other neuronally related categories within iNs, namely nicotine addiction and GABA (gamma-aminobutyric acid) receptor activity (Figure 3F).

Chromatin Accessibility Analysis

We examined chromatin accessibility using ATAC-Seq in 3 15q13.3 microdeletion lines and 3 control lines (Table S1 in Supplement 2). In iPSCs and iNs, the average chromatin accessibility log2 fold changes within the 15q13.3 region were −1.039 and −0.905, respectively, representing the loss of 1 copy number within the 15q13.3 region. PCA of the ATACSeq reads did not show a clear separation between 15q13.3 microdeletion cases and controls along PC1 or PC2 (Figure S2C, F in Supplement 1). Genome-wide, we identified 50 differentially accessible peaks in iPSCs and 72 peaks in iNs (Figure 4A, B and Tables

S10 and S11 in Supplement 2). These peaks were annotated to 9 promoter regions, 21 gene bodies, and 22 intergenic regions in iPSCs and to 14 promoter regions, 23 gene bodies, and 40 intergenic regions in iNs (Figure 4C, D).

We next examined transcription factor (TF) binding sites enriched in a list of differentially open promoters, generated as previously described (31). In iPSCs, 3 enriched motifs were associated with TFs (*ZNF711*, *MZF1*, and *MED1*) that were expressed in the same tissue (Figure 4E). In iNs, 5 expressed TFs (*MAX*, *ETV6*, *GRHL2*, *TWIST1*, and *SOX5*) associated with enriched motifs were similarly identified (Figure 4F). Of the 8 TFs associated with enriched motifs across iPSCs and iNs, 4 have been previously implicated in neuropsychiatric disorders. Variants in *ZNF711* and *MZF1* have been associated with intellectual disability and Alzheimer's disease (AD), respectively (48,49). Genetic variants in *SOX5* have been associated with a range of neuropsychiatric disorders, including major depressive disorder, (50), amyotrophic lateral sclerosis (51), AD (52), and intellectual disability (53). Lastly, *MAX* has been linked to depression-like behaviors in mouse models (54) and was found to be downregulated in cortex from patients with schizophrenia (55).

Correlation and Overlap Analysis Between Omics Layers

To analyze the relationships between the omics datasets, we calculated pairwise Pearson correlations between transcription, promoter-associated DNA methylation, and promoter-associated chromatin accessibility. Within each cell type, transcription and chromatin accessibility had a weak positive correlation (Figure 5A, D), transcription and DNA methylation had a weak negative correlation (Figure 5B, E), and DNA methylation and chromatin accessibility had a strong negative correlation (Figure 5C, F). These trends were consistent with the expected positive correlation between chromatin accessibility and transcription, the expected negative correlation between DNA methylation and transcription, and the expected negative correlation between DNA methylation and chromatin accessibility.

Despite the demonstrated linear correlation between the different omics datasets, the overlap in significant genes was limited. Only 15 genes were significant across at least 2 omics datasets in iPSCs, and 13 genes were significant across at least 2 datasets in iNs. One gene, *KCNH8*, was significant in all 3 iN omics analyses. *KCNH8* encodes a voltage-gated potassium channel that is primarily expressed in the nervous system (56). We also identified 4 genes that were significant in multiple omics datasets in both iPSCs and iNs. These genes, all of which have been implicated in studies of neuropsychiatric disorders, included *CNTN4*, a cell adhesion molecule associated with ASD (57) and schizophrenia (58); *PCDHGA10*, a member of the protocadherin family that has been implicated in schizophrenia and ASD (45); *SLC39A4*, a zinc transport protein regulated by *SHANK3*, a highly penetrant risk factor for ASD (59); and *SORCS1*, which alters amyloid precursor protein processing and is associated with AD (60).

Transcriptome-wide Effects of CRISPR Knockout of Individual 15q13.3 Microdeletion Genes

To evaluate the contributions of individual genes to the genome-wide expression changes observed in the 15q13.3 microdeletion samples, we generated CRISPR knockouts in 4 control iPSC lines targeting 5 of the genes located within the microdeletion: *CHRNA7*, *KLF13*, *OTUD7A*, *FAN1*, and *MTMR10* (Table S2 in Supplement 2). Two protein-coding genes in the CNV were excluded: 1) *TRPM1* because it is not expressed in iPSCs and iNs and 2) *ARHGAP11B* because its guide RNAs have off-target hits to its homolog *ARHGAP11A*. Because patients with homozygous deletions have been reported, usually with similar but more severe clinical phenotypes compared with those with heterozygous microdeletions, we selected homozygous single-gene knockouts, which were viable and would likely elicit stronger molecular phenotypes to assay (3). From the CRISPR iPSC lines, we generated day 6 iNs and performed RNA-Seq on them as previously described. As expected, PCA showed clustering primarily based on parental cell line identity (Figure S2G in Supplement 1). Genome-wide, we observed 3572 DE genes in the *FAN1* knockout, 223 DE genes in the *KLF13* knockout, 58 DE genes in the *MTMR10* knockout, 1 DE gene in the *OTUD7A* knockout, and no DE genes reaching significance in the *CHRNA7* knockout (Tables S12–S15 in Supplement 2). To compare the gene expression signatures in the 15q13.3 microdeletion and CRISPR knockout iNs, we performed pairwise correlation analyses. The 15q13.3 microdeletion iNs had a weak positive correlation with the *CHRNA7* and *OTUD7A* knockouts and had a moderate positive correlation with the *KLF13*, *FAN1*, and *MTMR10* knockouts (Figure S3A–E in Supplement 1).

Using WebGestalt, we performed GSEA on the CRISPR knockout RNA-Seq datasets. In the *CHRNA7* knockout, we observed GO terms related to transporter activity, which were likely related to the known function of *CHRNA7* as an ion channel that binds acetylcholine and mediates synaptic transmission (61,62). In addition, we saw an enrichment in the GOMF term Wnt–protein binding in the same direction as observed in the 15q13.3 iNs (Figure 6A). In the *KLF13* knockout, we observed GO terms related to DNA replication, neuron development, and tau protein kinase activity (Figure 6B). In both the *FAN1* and *MTMR10* knockouts, many of the top enriched GO terms were related to DNA binding. In addition, Wnt–protein binding was among the list of top 10 GOMF terms in the *MTMR10* knockout (Figure 6C, D). In the *OTUD7A* knockout, the top enriched GO terms were related to ribosome function but in the opposite direction from that observed in the 15q13.3 iNs. In addition, mitochondrial activity, which has been shown to be dysregulated in a number of neuropsychiatric disorders (63–66), was a prominent category in the *OTUD7A* knockout (Figure 6E).

Comparison With Mouse Model of 15q13.3 Microdeletion

We also compared the gene expression changes observed in our 15q13.3 microdeletion iNs with those reported by Gordon *et al.* in cortex from mice with hemizygous or homozygous deletions on mouse chromosome 7qC, a region highly syntenic to human 15q13.3 (67). Between the human iNs and mouse cortex, a weak positive correlation in gene expression was observed (Figure S4A, B in Supplement 1). After excluding CNV genes, no significant overlap remained between DE genes in iNs and mouse cortex. When we

performed GSEA on the mouse RNA-Seq dataset (67), we found one GOMF/GOBP term enriched in hemizygous deletion mice (GO:0042165 neurotransmitter binding), whereas the homozygous deletion mice had multiple enriched GO terms that were similar to those observed in our 15q13.3 microdeletion iNs related to Wnt signaling, DNA repair, and ribosome function. In addition, GO terms related to mitochondrial activity, which we observed in our *OTUD7A* knockouts, were highly enriched in the homozygous deletion mice (Table S16 in Supplement 2).

Sensitivity to Cisplatin-Induced DNA Damage

Because GO terms related to DNA binding and repair were strongly enriched in the 15q13.3 microdeletion iNs as well as in the *FAN1*, *MTMR10*, and *KLF13* knockout iNs, we evaluated cell survival after cisplatin-induced DNA damage in the 15q13.3 microdeletion and control iNs (Table S1 in Supplement 2). At a 0.5-mM cisplatin dose, we observed a much lower survival rate in 15q13.3 microdeletion iNs (56%) compared with control iNs (90%) (Figure 7). The significant difference in cell viability after cisplatin treatment provides further support for the observation from the RNA-Seq analysis that DNA repair pathways are disrupted in 15q13.3 microdeletion iNs.

DISCUSSION

Our multiomics analysis of 15q13.3 microdeletion iPSCs and iNs allowed us to interrogate the molecular impact of a large CNV that is strongly associated with a range of neuropsychiatric disorders such as schizophrenia and ASD. Large CNVs, while rare at the population level, typically have much larger effect sizes than other candidate loci and therefore are promising points of entry for understanding the associated disorders. Our current study investigated the 15q13.3 microdeletion as an important mutation in its own right and also demonstrated that iPSCs and iNs derived from carriers of such large CNVs can be used to identify molecular convergences between the main aberration and disease-relevant loci elsewhere in the genome.

Within the deletion region, all protein-coding genes, with the exception of nonexpressed *TRPM1*, had decreased expression in the 15q13.3 microdeletion samples, suggesting simple dosage sensitivity as a mechanism of action. We observed no significant changes in DNA methylation or chromatin accessibility within the deletion after accounting for the change in copy number, which was consistent with the lack of dosage compensation seen in the gene expression data. At the genome-wide level, we saw correlations of varying strengths between gene expression, DNA methylation, and chromatin accessibility. In both cell types, transcription and chromatin accessibility were positively correlated, whereas DNA methylation had a negative correlation with transcription and chromatin accessibility. The Pearson correlation between DNA methylation and chromatin accessibility was much stronger than their respective correlations with transcription. Both the direction and relative strength of correlation between these three omics layers were consistent with recent studies in mouse embryonic stem cells and human iPSC-derived neurons (68,69). We interpret these observations as signifying that different levels of functional genomics activity serve overlapping but distinct roles during cellular differentiation, where transcript levels are

highly sensitive to the functioning of the cell in its current state, while epigenetic marks are more stable indicators of the developmental trajectory.

Gene expression analysis in iNs compared with the analysis in iPSCs revealed a greater number of changes in neuropsychiatric disorder–related genes and pathways. Among the DE iN genes were *PRODH* and *DGCR6*, two major candidate genes for schizophrenia and autism located in the 22q11.2 microdeletion, which could be a further example of convergence between neuropsychiatric candidate loci (70). GO terms enriched in 15q13.3 iNs included several processes tied to abnormal neurodevelopment, including ribosome biogenesis, DNA binding and repair, and Wnt binding. The dysregulation of ribosome biogenesis has been implicated in neuropsychiatric disorders in previous studies of postmortem brains (71,72), olfactory neurosphere–derived cells (73), and neural progenitor cells (74). Similarly, the category of DNA binding and repair is known to play a key role in neuropsychiatric disorders, with mutations in DNA repair genes linked to schizophrenia and ASD (75). In addition, both apoptosis and oxidative stress, which are closely tied to DNA damage, have been implicated in a number of neuropsychiatric disorders (76–78). The disruption in DNA repair pathways observed in the RNA-Seq analysis was validated by the cisplatin assay, which showed a significant decrease in cell survival in 15q13.3 microdeletion iNs compared with control iNs after DNA damage. Another enriched GO category, Wnt signaling, plays a critical role in many neurodevelopmental processes, including synapse assembly, neuronal differentiation, and neurotransmission (79). Changes in the expression of Wnt pathway components are associated with several neurodevelopmental disorders including schizophrenia, bipolar disorder, and ASD (80,81). In addition to their enrichment in the 15q13.3 iNs, GO terms related to Wnt signaling, DNA binding, and ribosome function were also enriched in cortex from mouse models of homozygous 15q13.3 microdeletions, providing validation that these observed molecular signatures are generalizable for the 15q13.3 microdeletion and are not artifacts of the iPSC–iN model system. We also identified some limited convergence between our 15q13.3 CNV results and findings in other neuropsychiatric-associated CNVs (see Supplement 1 for details).

Our analysis of the epigenome revealed global reprogramming associated with the 15q13.3 microdeletion. Specifically, we identified differential methylation of protocadherins, a group of cell adhesion genes known to modulate the Wnt pathway (82,83). From the chromatin accessibility analysis, we identified several TFs with known connections to Wnt signaling, including *MZF1*, whose TF binding sites are enriched in promoters of Wnt pathway genes (84); *TWIST1*, which is activated by canonical Wnt signaling (85); and *SOX5*, which is associated with Wnt signaling activity in human SH-SY5Y neuroblastoma cells (52). In addition to the convergence on the Wnt signaling pathway, our multiomics analysis identified four genes (*CNTN4*, *PCDHGA10*, *SLC39A4*, and *SORCS1*) enriched in multiple omics datasets in both iPSCs and iNs, all of which have been previously associated with schizophrenia, ASD, or AD.

Multiple enriched GO terms identified in the 15q13.3 microdeletion iNs were also observed in the single-gene CRISPR knockout iNs. For example, Wnt binding was a significant GO term in both the *CHRNA7* and *MTMR10* knockouts. While *MTMR10* has not been linked to

Wnt signaling previously, several studies have implicated *CHRNA7* in the regulation of Wnt signaling, reporting that *CHRNA7* inhibitors block the nicotine-induced upregulation of Wnt signaling (86–88). GO terms related to ribosome function were enriched in the *OTUD7A* knockout. *OTUD7A* belongs to the ovarian tumor protease class of deubiquitinases, whose members (OTUD3 and OTUD6B) have been shown to act on translational machinery (89,90). Finally, GO terms related to DNA binding were enriched in the *FAN1*, *MTMR10*, and *KLF13* knockouts. *FAN1*, which encodes a nuclease that repairs DNA interstrand cross-links, plays a direct role in DNA repair (91–93). *MTMR10* encodes a catalytically inactive member of the myotubularin family. Although *MTMR10* itself has not been well studied, other members of the myotubularin family (*MTMR2* and *MTMR13*) have been identified in a DNA damage response screen (94,95). Lastly, *KLF13* is a transcription factor that may affect DNA binding through its known regulatory role in cell proliferation (96–100). On a general level, the CRISPR knockout results suggest that the disease-relevant effects of the 15q13.3 microdeletion are perhaps due not to the deletion of a single critical gene but rather to the combinatorial effects of several genes within the CNV boundaries. Supporting evidence for this multiple gene interaction model has also come from recent studies in other large CNVs associated with neuropsychiatric conditions (101,102).

In this study, we focused on a single neuronal cell type, earlystage iNs that can mature into excitatory projection neurons, in order to establish the viability and usefulness of this model system. Owing to the relative rareness of the CNV and the laborintensive nature of iPSC–iN work, the study cohort was limited to 3 15q13.3 deletion patients and 3 control subjects who were sex matched but were not perfectly matched with regard to exact age and ethnicity. However, we were still able to identify disrupted pathways that converged across different experimental approaches and omics layers within our study as well as with previous studies of neuropsychiatric disorders. With the validation provided by the mouse model reanalysis and by the CRISPR knockout experiments, which eliminated confounding factors resulting from differences in genetic background, we expect that the molecular effects we describe form part of a common thread in the early pathogenesis of the 15q13.3 microdeletion syndrome. Interindividual genetic variance, which is considerable between deletion carriers and modifies the molecular effects of the deletion, needs to be further dissected in studies using larger cohorts as well as in cells differentiated into other neuronal and glial types. Beyond the analysis of the 15q13.3 microdeletion, our study provides a blueprint for assaying the molecular consequences of neuropsychiatric-associated chromosomal aberrations. The many points of convergence with genes and pathways already implicated in neuronal dysfunction underline how the study of variants such as the 15q13.3 microdeletion can inform our general understanding of the molecular basis of neuropsychiatric disorders.

Supplementary Material

Refer to Web version on PubMed Central for supplementary material.

ACKNOWLEDGMENTS AND DISCLOSURES

This work was supported by the National Science Foundation (to SZ), the National Institutes of Health (Grant Nos. 5P50HG007735–05 [to AEU and WHW], 1R01HG010359–01A1 [to WHW], and 1DP2MH100010–01 [to AEU]),

and the March of Dimes Foundation (Grant No. 6-FY13–142 [to AEU]). AEU is a Tashia and John Morgridge Faculty Scholar at the Stanford Child Health Research Institute. The Urban Lab received funding from Bruce Blackie and William McIvor.

SZ and AEU designed the study. SZ, XZ, SM, and WHW developed the analysis pipeline. SZ, JAB, JH, AS, RP, MH, YH, CP, and KD contributed to cell line generation and characterization. SZ and MH performed the sequencing experiments. SZ and SM carried out the data analysis. SZ and AEU interpreted the data and wrote the manuscript.

We thank Guangwen Wang from the Stanford Stem Cell Core for the generation of iPSCs and Javier Fernandez Alcudia from the Stanford Gene Vector and Virus Core for the production of lentiviruses for neurogenin-2 induction. We also thank Xiaowei Zhu for advice on data analysis. We acknowledge helpful discussions with Michael Talkowski, Rachita Yadav, and Derek Tai as well as with Bruce Blackie and William McIvor.

The datasets generated and analyzed in the current study are available at National Center for Biotechnology Information (NCBI) Gene Expression Omnibus GSE135131 (token whobqkaghtyjbkf) and NCBI Sequence Read Archive PRJNA557485.

REFERENCES

1. van Bon BWM, Mefford HC, Menten B, Koolen DA, Sharp AJ, Nillesen WM, et al. (2009): Further delineation of the 15q13 microdeletion and duplication syndromes: A clinical spectrum varying from non-pathogenic to a severe outcome. J Med Genet 46:511–523. [PubMed: 19372089]
2. Sharp AJ, Mefford HC, Li K, Baker C, Skinner C, Stevenson RE, et al. (2008): A recurrent 15q13.3 microdeletion syndrome associated with mental retardation and seizures. Nat Genet 40:322–328. [PubMed: 18278044]
3. Lowther C, Costain G, Stavropoulos DJ, Melvin R, Silversides CK, Andrade DM, et al. (2015): Delineating the 15q13.3 microdeletion phenotype: A case series and comprehensive review of the literature. Genet Med 17:149–157. [PubMed: 25077648]
4. Cubells JF, Deoreo EH, Harvey PD, Garlow SJ, Garber K, Adam MP, et al. (2011): Pharmaco-genetically guided treatment of recurrent rage outbursts in an adult male with 15q13.3 deletion syndrome. Am J Med Genet A 155:805–810.
5. Gillentine MA, Yin J, Bajic A, Zhang P, Cummock S, Kim JJ, et al. (2017): Functional consequences of CHRNA7 copy-number alterations in induced pluripotent stem cells and neural progenitor cells. Am J Hum Genet 101:874–887. [PubMed: 29129316]
6. Freedman R, Hall M, Adler LE, Leonard S (1995): Evidence in postmortem brain tissue for decreased numbers of hippocampal nicotinic receptors in schizophrenia. Biol Psychiatry 38:22–33. [PubMed: 7548469]
7. Ray MA, Graham AJ, Lee M, Perry RH, Court JA, Perry EK (2005): Neuronal nicotinic acetylcholine receptor subunits in autism: An immunohistochemical investigation in the thalamus. Neurobiol Dis 19:366–377. [PubMed: 16023579]
8. Thomsen MS, Weyn A, Mikkelsen JD (2011): Hippocampal α7 nicotinic acetylcholine receptor levels in patients with schizophrenia, bipolar disorder, or major depressive disorder. Bipolar Disord 13:701–707. [PubMed: 22085484]
9. Uddin M, Unda BK, Kwan V, Holzapfel NT, White SH, Chalil L, et al. (2018): OTUD7A regulates neurodevelopmental phenotypes in the 15q13.3 microdeletion syndrome. Am J Hum Genet 102:278–295. [PubMed: 29395074]
10. Yin J, Chen W, Chao ES, Soriano S, Wang L, Wang W, et al. (2018): Otud7a Knockout Mice Recapitulate Many Neurological Features of 15q13.3 Microdeletion Syndrome. Am J Hum Genet 102:296–308. [PubMed: 29395075]
11. Ionita-Laza I, Xu B, Makarov V, Buxbaum JD, Roos JL, Gogos JA, et al. (2014): Scan statistic-based analysis of exome sequencing data identifies FAN1 at 15q13.3 as a susceptibility gene for schizophrenia and autism. Proc Natl Acad Sci U S A 111:343–348. [PubMed: 24344280]
12. Zhou W, Otto EA, Cluckey A, Airik R, Hurd TW, Chaki M, et al. (2013): FAN1 mutations cause karyomegalic interstitial nephritis, linking chronic kidney failure to defective DNA damage repair. Nat Genet 44:910–915.

13. Florio M, Albert M, Taverna E, Namba T, Brandl H, Lewitus E, et al. (2015): Human-specific gene ARHGAP11B promotes basal progenitor amplification and neocortex expansion. Science 347:1465–1470. [PubMed: 25721503]
14. Le Pichon J-B, Yu S, Kibiryeva N, Graf WD, Bittel DC (2013): Genome-wide gene expression in a patient with 15q13.3 homozygous microdeletion syndrome. Eur J Hum Genet 21:1093–1099. [PubMed: 23361223]
15. Kuehner JN, Bruggeman EC, Wen Z, Yao B (2019): Epigenetic regulations in neuropsychiatric disorders. Front Genet 10:1–30. [PubMed: 30804975]
16. Zhang Y, Pak C, Han Y, Ahlenius H, Zhang Z, Marro S, et al. (2013): Rapid single-step induction of functional neurons from human pluripotent stem cells 2013;. 78:785–798.
17. Li H, Durbin R (2010): Fast and accurate long-read alignment with Burrows-Wheeler transform. Bioinformatics 26:589–595. [PubMed: 20080505]
18. Quinlan AR, Hall IM (2010): BEDTools: A flexible suite of utilities for comparing genomic features. Bioinformatics 26:841–842. [PubMed: 20110278]
19. Abyzov A, Urban AE, Snyder M, Gerstein M (2011): CNVnator: An approach to discover, genotype, and characterize typical and atypical CNVs from family and population genome sequencing. Genome Res 21:974–984. [PubMed: 21324876]
20. Trapnell C, Pachter L, Salzberg SL (2009): TopHat: Discovering splice junctions with RNA-Seq. Bioinformatics 25:1105–1111. [PubMed: 19289445]
21. Love MI, Huber W, Anders S (2014): Moderated estimation of fold change and dispersion for RNA-seq data with DESeq2. Genome Biol 15:550. [PubMed: 25516281]
22. Wang J, Vasaikar S, Shi Z, Greer M, Zhang B (2017): WebGestalt 2017: A more comprehensive, powerful, flexible and interactive gene set enrichment analysis toolkit. Nucleic Acids Res 45:130–137.
23. Langmead B, Salzberg SL (2012): Fast gapped-read alignment with Bowtie 2. Nat Methods 9:357–359. [PubMed: 22388286]
24. Krueger F, Andrews SR (2011): Bismark: A flexible aligner and methylation caller for Bisulfite-Seq applications. Bioinformatics 27:1571–1572. [PubMed: 21493656]
25. Li S, Figueroa ME, Kormaksson M, Melnick A, Mason CE, Garrett-Bakelman FE, et al. (2012): methylKit: A comprehensive R package for the analysis of genome-wide DNA methylation profiles. Genome Biol 13:R87. [PubMed: 23034086]
26. Jühling F, Kretzmer H, Bernhart SH, Otto C, Stadler PF, Hoffmann S (2016): Metilene: Fast and sensitive calling of differentially methylated regions from bisulfite sequencing data. Genome Res 26:256–262. [PubMed: 26631489]
27. Buenrostro JD, Giresi PG, Zaba LC, Chang HY, Greenleaf WJ (2013): Transposition of native chromatin for fast and sensitive epigenomic profiling of open chromatin, DNA-binding proteins and nucleosome position. Nat Methods 10:1213–1218. [PubMed: 24097267]
28. Bernstein BE, Brown M, Johnson DS, Liu XS, Nussbaum C, Myers RM, et al. (2008): Model-based analysis of ChIP-Seq (MACS). Genome Biol 9:R137. [PubMed: 18798982]
29. Stark R, Brown G (2011): DiffBind: Differential binding analysis of ChIP-Seq peak data Available at: http://bioconductor.org/packages/release/bioc/vignettes/DiffBind/inst/doc/DiffBind.pdf. Accessed June 1, 2020.
30. Heinz S, Benner C, Spann N, Bertolino E, Lin YC, Laslo P, et al. (2010): Simple combinations of lineage-determining transcription factors prime cis-regulatory elements required for macrophage and B cell identities. Mol Cell 38:576–589. [PubMed: 20513432]
31. Duren Z, Chen X, Jiang R, Wang Y, Wong WH (2017): Modeling gene regulation from paired expression and chromatin accessibility data. Proc Natl Acad Sci U S A 114:E4914–E4923. [PubMed: 28576882]
32. Bateman A, Martin MJ, O'Donovan C, Magrane M, Alpi E, Antunes R, et al. (2017): UniProt: The universal protein knowledgebase. Nucleic Acids Res 45:D158–D169. [PubMed: 27899622]
33. Levinson DF, Duan J, Oh S, Wang K, Sanders AR, Shi J, et al. (2011): Copy number variants in schizophrenia: Confirmation of five previous findings and new evidence for 3q29 microdeletions and VIPR2 duplications. Am J Psychiatry 168:302–316. [PubMed: 21285140]

34. Vacic V, McCarthy S, Malhotra D, Murray F, Chou H-H, Peoples A, et al. (2011): Duplications of the neuropeptide receptor gene VIPR2 confer significant risk for schizophrenia. Nature 471:499–503. [PubMed: 21346763]
35. Corbett MA, Bellows ST, Li M, Carroll R, Micallef S, Carvill GL, et al. (2016): Dominant KCNA2 mutation causes episodic ataxia and pharmacoresponsive epilepsy. Neurology 87:1975–1984. [PubMed: 27733563]
36. Everett K, Chioza B, Aicardi J, Aschauer H, Brouwer O, Covanis A, et al. (2008): Europe PMC funders group linkage and association analysis of CACNG3 in childhood absence epilepsy 2008;. 15:463–472.
37. Hammer MF, Wagnon JL, Mefford HC, Meisler MH (1993): SCN8A-related epilepsy with encephalopathy Available at: http://www.ncbi.nlm.nih.gov/pubmed/27559564. Accessed June 1, 2020.
38. Tanaka AJ, Cho MT, Millan F, Juusola J, Retterer K, Joshi C, et al. (2015): Mutations in SPATA5 are associated with microcephaly, intellectual disability, seizures, and hearing loss. Am J Hum Genet 97:457–464. [PubMed: 26299366]
39. Ahmed I, Buchert R, Zhou M, Jiao X, Mittal K, Sheikh TI, et al. (2015): Mutations in DCPS and EDC3 in autosomal recessive intellectual disability indicate a crucial role for mRNA decapping in neurodevelopment. Hum Mol Genet 24:3172–3180. [PubMed: 25701870]
40. Ng CKL, Shboul M, Taverniti V, Bonnard C, Lee H, Eskin A, et al. (2015): Loss of the scavenger mRNA decapping enzyme DCPS causes syndromic intellectual disability with neuromuscular defects. Hum Mol Genet 24:3163–3171. [PubMed: 25712129]
41. Sheth J, Ranjan G, Shah K, Bhavsar R, Sheth F (2017): Novel LINS1 missense mutation in a family with non-syndromic intellectual disability. Am J Med Genet A 173:1041–1046. [PubMed: 28181389]
42. Liu H, Heath SC, Sobin C, Roos JL, Galke BL, Blundell ML, et al. (2002): Genetic variation at the 22q11 PRODH2/DGCR6 locus presents an unusual pattern and increases susceptibility to schizophrenia. Proc Natl Acad Sci U S A 99:3717–3722. [PubMed: 11891283]
43. Guilmatre A, Dubourg C, Mosca A-L, Legallic S, Goldenberg A, Drouin-Garraud V, et al. (2009): Recurrent rearrangements in synaptic and neurodevelopmental genes and shared biologic pathways in schizophrenia, autism, and mental retardation. Arch Gen Psychiatry 66:947–956. [PubMed: 19736351]
44. Piazzi M, Bavelloni A, Gallo A, Faenza I, Blalock WL (2019): Signal Transduction in Ribosome Biogenesis: A Recipe to Avoid Disaster. Int J Mol Sci 20:2718.
45. Men K, Weiner JA (2017): Regulation of Wnt signaling by protocadherins. Semin Cell Dev Biol 69:158–171. [PubMed: 28774578]
46. Hajj NE, Dittrich M, Haaf T (2017): Epigenetic dysregulation of protocadherins in human disease. Semin Cell Dev Biol 69:172–182. [PubMed: 28694114]
47. Ward TR, Zhang X, Leung LC, Zhou B, Muench K, Roth JG, et al. (2020): Genome-wide molecular effects of the neuropsychiatric 16p11 CNVs in an iPSC-to-iN neuronal model. bioRxiv. 10.1101/2020.02.09.940965.
48. Porcellini E, Carbone I, Martelli PL, Ianni M, Casadio R, Pession A, et al. (2013): Haplotype of single nucleotide polymorphisms in exon 6 of the MZF-1 gene and Alzheimer's disease. J Alzheimers Dis 34:439–447. [PubMed: 23241556]
49. van der Werf IM, Van Dijck A, Reyniers E, Helsmoortel C, Kumar AA, Kalscheuer VM, et al. (2017): Mutations in two large pedigrees highlight the role of ZNF711 in X-linked intellectual disability. Gene 605:92–98. [PubMed: 27993705]
50. Wray NR, Ripke S, Mattheisen M, Trzaskowski M, Byrne EM, Abdellaoui A, et al. (2018): Genome-wide association analyses identify 44 risk variants and refine the genetic architecture of major depression. Nat Genet 50:668–681. [PubMed: 29700475]
51. Daoud H, Valdmanis PN, Gros-Louis F, Belzil V, Spiegelman D, Henrion E, et al. (2011): Resequencing of 29 candidate genes in patients with familial and sporadic amyotrophic lateral sclerosis. Arch Neurol 68:587–593. [PubMed: 21220648]

52. Li A, Hooli B, Mullin K, Tate RE, Bubnys A, Kirchner R, et al. (2017): Silencing of the Drosophila ortholog of SOX5 leads to abnormal neuronal development and behavioral impairment. Hum Mol Genet 26:1472–1482. [PubMed: 28186563]
53. Lamb AN, Rosenfeld JA, Neill NJ, Talkowski ME, Blumenthal I, Girirajan S, et al. (2012): Haploinsufficiency of SOX5 at 12p12.1 is associated with developmental delays with prominent language delay, behavior problems, and mild dysmorphic features. Hum Mutat 33:728–740. [PubMed: 22290657]
54. Resende LS, Amaral CE, Soares RBS, Alves AS, Alves-Dos-Santos L, Britto LRG, et al. (2016): Social stress in adolescents induces depression and brain-region-specific modulation of the transcription factor MAX. Transl Psychiatry 6:e914.
55. Novikova SI, He F, Cutrufello NJ, Lidow MS (2006): Identification of protein biomarkers for schizophrenia and bipolar disorder in the postmortem prefrontal cortex using SELDI-TOF-MS ProteinChip profiling combined with MALDI-TOF-PSD-MS analysis. Neurobiol Dis 23:61–76. [PubMed: 16549361]
56. Zou A, Lin Z, Humble M, Creech CD, Wagoner PK, Krafte D, et al. (2003): Distribution and functional properties of human KCNH8 (Elk1) potassium channels. Am J Physiol Cell Physiol 285:C1356–C1366. [PubMed: 12890647]
57. Cottrell CE, Bir N, Varga E, Alvarez CE, Bouyain S, Zernzach R, et al. (2011): Contactin 4 as an autism susceptibility locus. Autism Res 4:189–199. [PubMed: 21308999]
58. Liu M, Malone SM, Vaidyanathan U, Keller MC, Abecasis G, McGue M, et al. (2017): Psychophysiological endophenotypes to characterize mechanisms of known schizophrenia genetic loci. Psychol Med 47:1116–1125. [PubMed: 27995817]
59. Pfaender S, Sauer AK, Hagmeyer S, Mangus K, Linta L, Liebau S, et al. (2017): Zinc deficiency and low enterocyte zinc transporter expression in human patients with autism related mutations in SHANK3. Sci Rep 7:45190. [PubMed: 28345660]
60. Lane RF,St George-Hyslop P, Hempstead BL, Small SA, Strittmatter SM, Gandy S (2012): Vps10 family proteins and the retromer complex in aging-related neurodegeneration and diabetes. J Neurosci 32:14080–14086. [PubMed: 23055476]
61. Uteshev VV, Meyer EM, Papke RL (2003): Regulation of neuronal function by choline and 4OH-GTS-21 through alpha 7 nicotinic receptors. J Neurophysiol 89:1797–1806. [PubMed: 12611953]
62. Changeux J-P (2012): The nicotinic acetylcholine receptor: The founding father of the pentameric ligand-gated ion channel superfamily. Jf Biol Chem 287:40207–40215.
63. Prabakaran S, Swatton JE, Ryan MM, Huffaker SJ, Huang JT-J, Griffin JL, et al. (2004): Mitochondrial dysfunction in schizophrenia: Evidence for compromised brain metabolism and oxidative stress. Mol Psychiatry 9:684–697. [PubMed: 15098003]
64. Shao L, Martin MV, Watson SJ, Schatzberg A, Akil H, Myers RM, et al. (2008): Mitochondrial involvement in psychiatric disorders. Ann Med 40:281–295. [PubMed: 18428021]
65. Rosenfeld M, Brenner-Lavie H, Ari SG-B, Kavushansky A, BenShachar D (2011): Perturbation in mitochondrial network dynamics and in complex I dependent cellular respiration in schizophrenia. Biol Psychiatry 69:980–988. [PubMed: 21397211]
66. Cruz ACP, Ferrasa A, Muotri AR, Herai RH (2019): Frequency and association of mitochondrial genetic variants with neurological disorders. Mitochondrion 46:345–360. [PubMed: 30218715]
67. Gordon A, Forsingdal A, Klewe IV, Nielsen J, Didriksen M, Werge T, et al. (2019): Transcriptomic networks implicate neuronal energetic abnormalities in three mouse models harboring autism and schizophrenia-associated mutations [published online ahead of print Nov 8]. Mol Psychiatry.
68. Clark SJ, Argelaguet R, Kapourani CA, Stubbs TM, Lee HJ, AldaCatalinas C, et al. (2018): ScNMT-seq enables joint profiling of chromatin accessibility DNA methylation and transcription in single cells. Nat Commun 9:781. [PubMed: 29472610]
69. Zhang S, Moy W, Zhang H, Leites C, McGowan H, Shi J, et al. (2018): Open chromatin dynamics reveals stage-specific transcriptional networks in hiPSC-based neurodevelopmental model. Stem Cell Res 29:88–98. [PubMed: 29631039]
70. Lin M, Pedrosa E, Hrabovsky A, Chen J, Puliafito BR, Gilbert SR, et al. (2016): Integrative transcriptome network analysis of iPSC-derived neurons from schizophrenia and schizoaffective disorder patients with 22q11.2 deletion. BMC Syst Biol 10:105. [PubMed: 27846841]

71. Darby MM, Yolken RH, Sabunciyan S (2016): Consistently altered expression of gene sets in postmortem brains of individuals with major psychiatric disorders. Transl Psychiatry 6:e890.
72. Ning LF, Yu YQ, Guoji ET, Kou CG, Wu YH, Shi JP (2015): Metaanalysis of differentially expressed genes in autism based on gene expression data 2015;. 14:2146–2155.
73. English JA, Fan Y, Föcking M, Lopez LM, Hryniewiecka M, Wynne K, et al. (2015): Reduced protein synthesis in schizophrenia patientderived olfactory cells. Transl Psychiatry 5:e663.
74. Topol A, English JA, Flaherty E, Rajarajan P, Hartley BJ, Gupta S, et al. (2015): Increased abundance of translation machinery in stem cell-derived neural progenitor cells from four schizophrenia patients. Transl Psychiatry 5:e662.
75. Markkanen E, Meyer U, Dianov GL (2016): DNA damage and repair in schizophrenia and autism: Implications for cancer comorbidity and beyond. Int J Mol Sci 17:856.
76. Raza MU, Tufan T, Wang Y, Hill C, Zhu M-Y (2016): DNA damage in major psychiatric diseases. Neurotox Res 30:251–267. [PubMed: 27126805]
77. Chailangkarn T, Trujillo CA, Freitas BC, Hrvoj-Mihic B, Herai RH, Yu DX, et al. (2016): A human neurodevelopmental model for Williams syndrome. Nature 536:338–343. [PubMed: 27509850]
78. Lewis EMA, Meganathan K, Baldridge D, Gontarz P, Zhang B, Bonni A, et al. (2019): Cellular and molecular characterization of multiplex autism in human induced pluripotent stem cell-derived neurons. Mol Autism 10:51. [PubMed: 31893020]
79. Inestrosa NC, Varela-Nallar L (2014): Wnt signaling in the nervous system and in Alzheimer's disease. J Mol Cell Biol 6:64–74. [PubMed: 24549157]
80. Hussaini SMQ, Choi CI, Cho CH, Kim HJ, Jun H, Jang MH (2014): Wnt signaling in neuropsychiatric disorders: Ties with adult hippocampal neurogenesis and behavior. Neurosci Biobehav Rev 47:369–383. [PubMed: 25263701]
81. Topol A, Zhu S, Tran N, Simone A, Fang G, Brennand KJ (2015): Altered WNT signaling in human induced pluripotent stem cell neural progenitor cells derived from four schizophrenia patients. Biol Psychiatry 78:e29–e34. [PubMed: 25708228]
82. Chen J, Lu Y, Meng S, Han M-H, Lin C, Wang X (2008): alpha- and gamma-Protocadherins negatively regulate PYK2. J Biol Chem 284:2880–2890. [PubMed: 19047047]
83. Suo L, Lu H, Ying G, Capecchi MR, Wu Q (2012): Protocadherin clusters and cell adhesion kinase regulate dendrite complexity through Rho GTPase. J Mol Cell Biol 4:362–376. [PubMed: 22730554]
84. McKay GJ, Kavanagh DH, Crean JK, Maxwell AP (2016): Bioinformatic evaluation of transcriptional regulation of WNT pathway genes with reference to diabetic nephropathy. J Diabetes Res 2016 7684038.
85. Reinhold MI, Kapadia RM, Liao Z, Naski MC (2006): The Wnt-inducible transcription factor Twist1 inhibits chondrogenesis. J Biol Chem 281:1381–1388. [PubMed: 16293629]
86. Sakurai R, Cerny LM, Torday JS, Rehan VK (2011): Mechanism for nicotine-induced up-regulation of Wnt signaling in human alveolar interstitial fibroblasts. Exp Lung Res 37:144–154. [PubMed: 21133803]
87. Inestrosa NC, Godoy JA, Vargas JY, Arrazola MS, Rios JA, Carvajal FJ, et al. (2013): Nicotine prevents synaptic impairment induced by amyloid-b oligomers through a7-nicotinic acetylcholine receptor activation. Neuromol Med 15:549–569.
88. Liu Y, Hao S, Yang B, Fan Y, Qin X, Chen Y, et al. (2017): Wnt/βcatenin signaling plays an essential role in a7 nicotinic receptormediated neuroprotection of dopaminergic neurons in a mouse Parkinson's disease model. Biochem Pharmacol 140:115–123. [PubMed: 28551099]
89. Sobol A, Askonas C, Alani S, Weber MJ, Ananthanarayanan V, Osipo C, et al. (2017): Deubiquitinase OTUD6B isoforms are important regulators of growth and proliferation. Mol Cancer Res 15:117–127. [PubMed: 27864334]
90. Garshott DM, Sundaramoorthy E, Leonard M, Bennett EJ (2020): Distinct regulatory ribosomal ubiquitylation events are reversible and hierarchically organized. eLife 9:e54023.
91. Liu T, Ghosal G, Yuan J, Chen J, Huang J (2010): FAN1 acts with FANCI-FANCD2 to promote DNA interstrand cross-link repair. Science 329:693–696. [PubMed: 20671156]

92. Yoshikiyo K, Kratz K, Hirota K, Nishihara K, Takata M, Kurumizaka H, et al. (2010): KIAA1018/FAN1 nuclease protects cells against genomic instability induced by interstrand cross-linking agents. Proc Natl Acad Sci U S A 107:21553–21557. [PubMed: 21115814]

93. Smogorzewska A, Desetty R, Saito TT, Schlabach M, Lach FP, Sowa ME, et al. (2010): A genetic screen identifies FAN1, a Fanconi anemia-associated nuclease necessary for DNA interstrand crosslink repair. Mol Cell 39:36–47. [PubMed: 20603073]

94. Wishart MJ, Dixon JE (2002): PTEN and myotubularin phosphatases: From 3-phosphoinositide dephosphorylation to disease. Trends Cell Biol 12:579–585. [PubMed: 12495846]

95. Paulsen RD, Soni DV, Wollman R, Hahn AT, Yee M-C, Guan A, et al. (2009): A genome-wide siRNA screen reveals diverse cellular processes and pathways that mediate genome stability. Mol Cell 35:228–239. [PubMed: 19647519]

96. Lavallée G, Andelfinger G, Nadeau M, Lefebvre C, Nemer G, Horb ME, et al. (2006): The Kruppel-like transcription factor KLF13 is a novel regulator of heart development. EMBO J 25:5201–5213. [PubMed: 17053787]

97. Nemer M, Horb ME (2007): The KLF family of transcriptional regulators in cardiomyocyte proliferation and differentiation. Cell Cycle 6:117–121. [PubMed: 17245133]

98. Chen C-P, Chen C-Y, Chern S-R, Wu P-S, Chen S-W, Wu F-T, et al. (2019): Detection of de novo del(18)(q22.2) and a familial of 15q13.2q13.3 microduplication in a fetus with congenital heart defects. Taiwan J Obstet Gynecol 58:704–708. [PubMed: 31542097]

99. Lin C-Z, Qi B-R, Hu J-S, Huang Y-D, Huang X-Q (2019): Chromosome 15q13 microduplication in a fetus with cardiac rhabdomyoma: A case report. Mol Cytogenet 12:24. [PubMed: 31149030]

100. Song A, Chen Y-F, Thamatrakoln K, Storm TA, Krensky AM (1999): RFLAT-1: A new zinc finger transcription factor that activates RANTES gene expression in T lymphocytes. Immunity 10:93–103. [PubMed: 10023774]

101. Jensen M, Girirajan S (2019): An interaction-based model for neuropsychiatric features of copy-number variants. PLoS Genet 15: e1007879.

102. Qiu Y, Arbogast T, Lorenzo SM, Li H, Tang SC, Richardson E, et al. (2019): Oligogenic effects of 16p11.2 copy-number variation on craniofacial development. Cell Rep 28:3320–3328.e4.

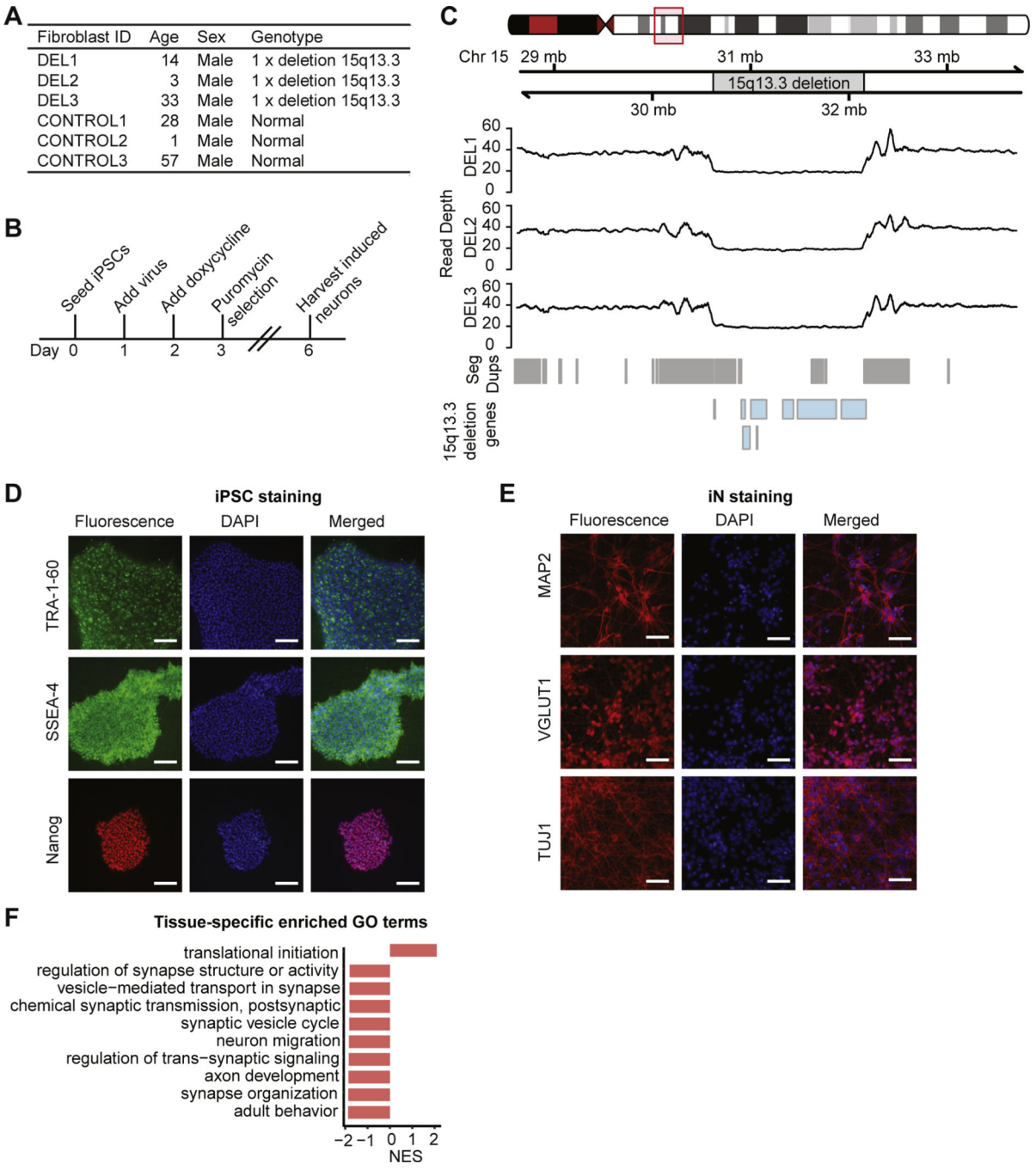

Figure 1.

Generation and characterization of CNV lines. (**A**) Information on donors of fibroblasts, including age, sex, and genotype. (**B**) Induced neuron generation timeline. (**C**) Sequencing read depth of fibroblast samples. (**D**) Immunocytochemistry for the pluripotency markers Nanog, TRA-1–60, and SSEA-4 on iPSCs (scale bar = 200 μm). (**E**) Immunocytochemistry for the neuronal markers MAP2, VGLUT1, and TUJ1 on day 6–induced neurons (scale bar = 200 μm). (**F**) Top 10 GO biological process terms from gene set enrichment analysis of genes differentially expressed between iPSCs and iNs, ordered by NES. Chr, chromosome;

CNV, copy number variant; GO, Gene Ontology; iN, induced neuron; iPSC, induced pluripotent stem cell; NES, normalized enrichment score.

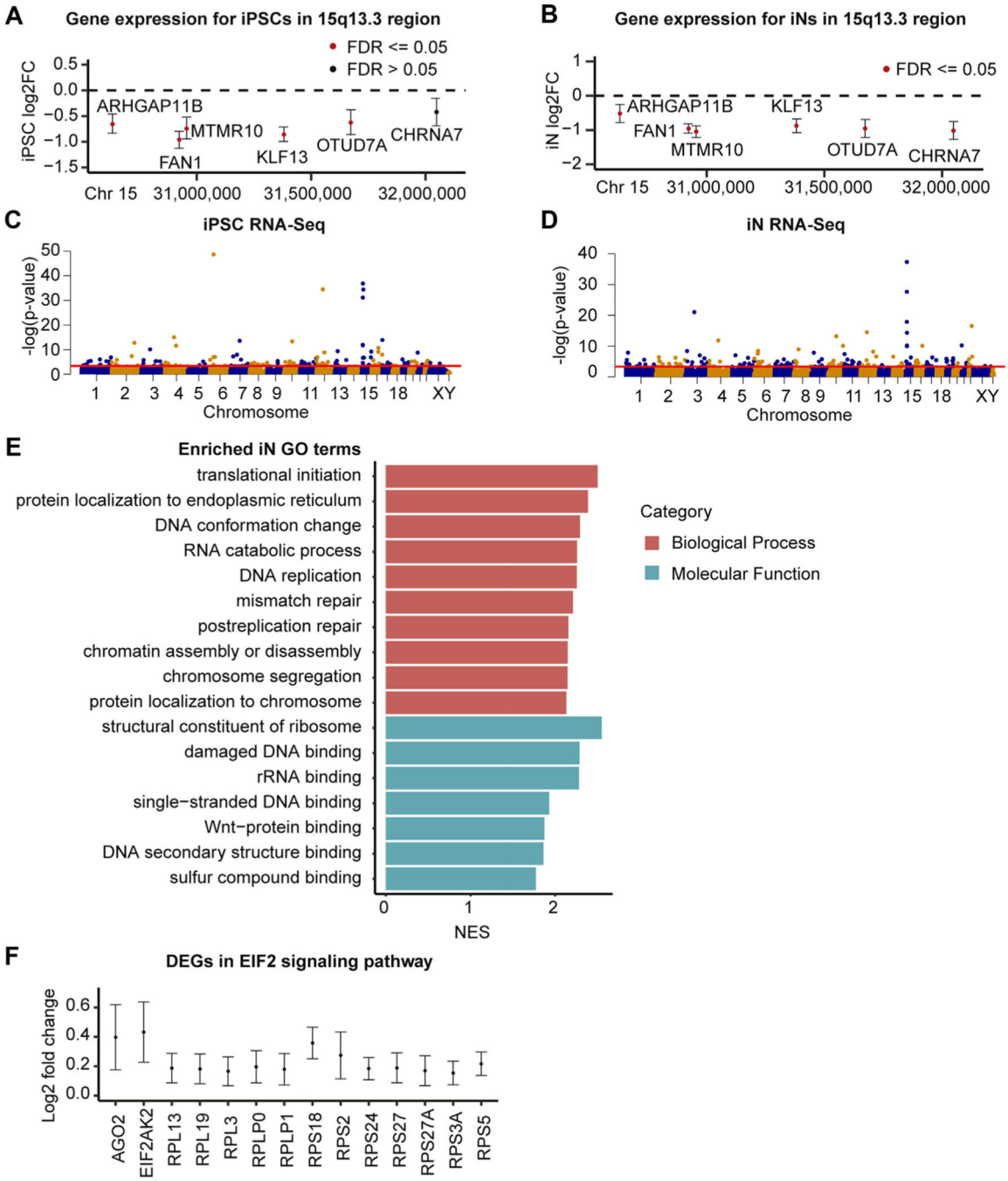

Figure 2.

Gene expression changes within the 15q13.3 microdeletion and genome wide. (**A, B**) Log2 FC of protein-coding 15q13.3 genes in deletion samples compared with control subjects in iPSCs (**A**) and iNs (**B**) (95% confidence intervals shown). (**C**, **D**) Manhattan plots of RNA-Seq genes in iPSCs (**C**) and iNs (**D**), with the red threshold line indicating .05 FDR significance. (**E**) Significant GO terms from gene set enrichment analysis of 15q13.3 iN RNA-Seq dataset. The top 10 terms in each category based on FDR are listed, ordered by NES. (**F**) Log2 FC of EIF2 signaling genes differentially expressed in deletion iNs

compared with control iNs (95% confidence intervals shown). Chr, chromosome; DEG, differentially expressed gene; FC, fold change; FDR, false discovery rate; GO, Gene Ontology; iN, induced neuron; iPSC, induced pluripotent stem cell; NES, normalized enrichment score; rRNA, ribosomal RNA; RNA-Seq, RNA sequencing.

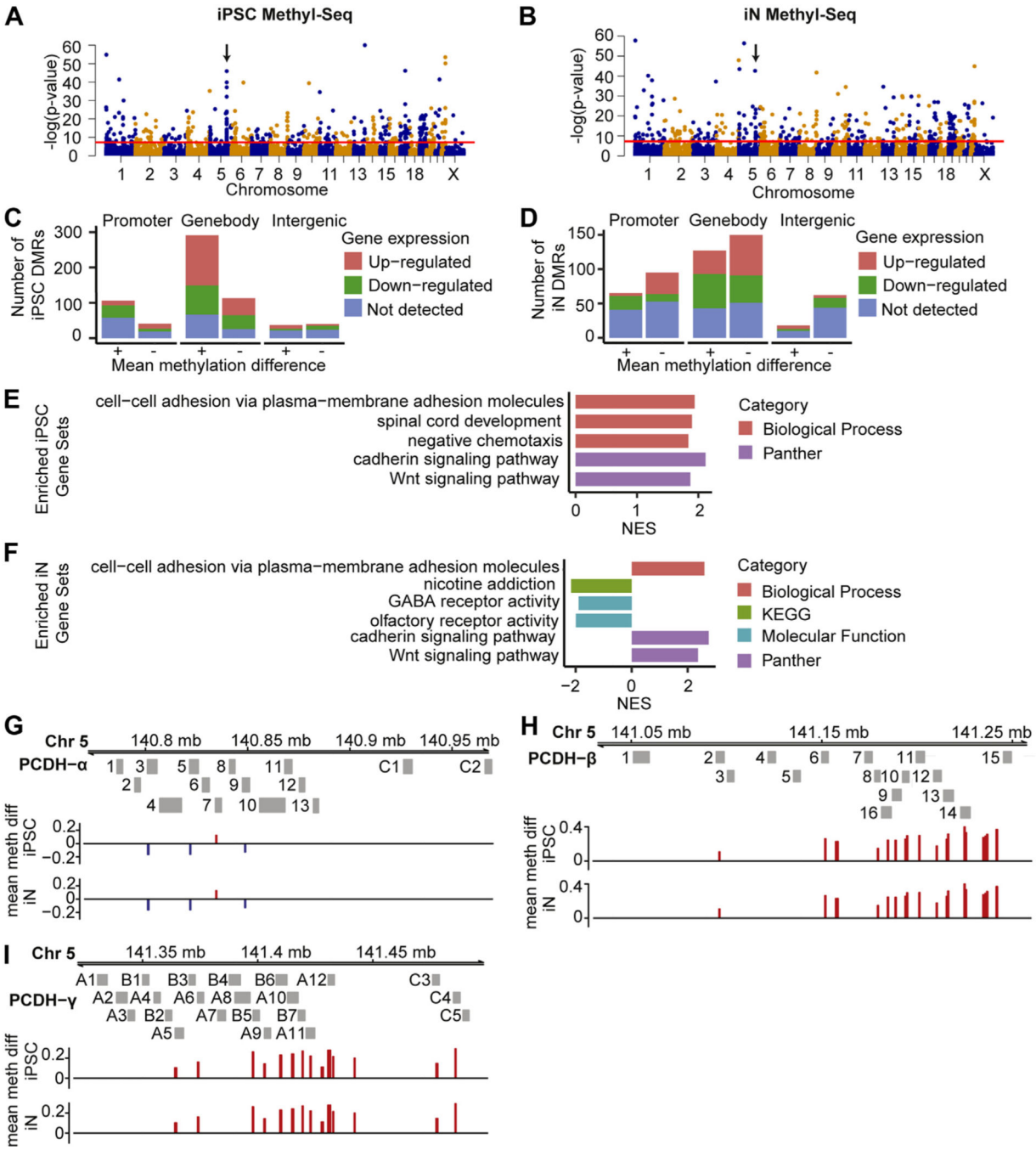

Figure 3.

DMRs in 15q13.3 microdeletion lines. (**A**, **B**) Genome-wide distribution of DMRs in iPSCs (**A**) and iNs (**B**). DMRs above red threshold line have ≥0.1 mean methylation difference and adjusted p ≤ .05. Arrows indicate PCDH gene clusters. (**C**, **D**) DMRs in iPSCs and iNs, split by DMR location, direction of mean methylation difference, and direction of expression change in nearest gene. (**E**, **F**) Significant terms from gene set enrichment analysis of 15q13.3 iN and iPSC Methyl-Seq datasets, sorted by NES. (**G–I**) DMRs located near the alpha (**G**), beta (**H**), and gamma (**I**) PCDH families. DMRs are colored red for

higher mean methylation, and blue for lower mean methylation, in deletion samples. Chr, chromosome; DMR, differentially methylated region; GABA, gammaaminobutyric acid; iN, induced neuron; iPSC, induced pluripotent stem cell; Methyl-Seq, DNA methylation sequencing; NES, normalized enrichment score; PCDH, protocadherin.

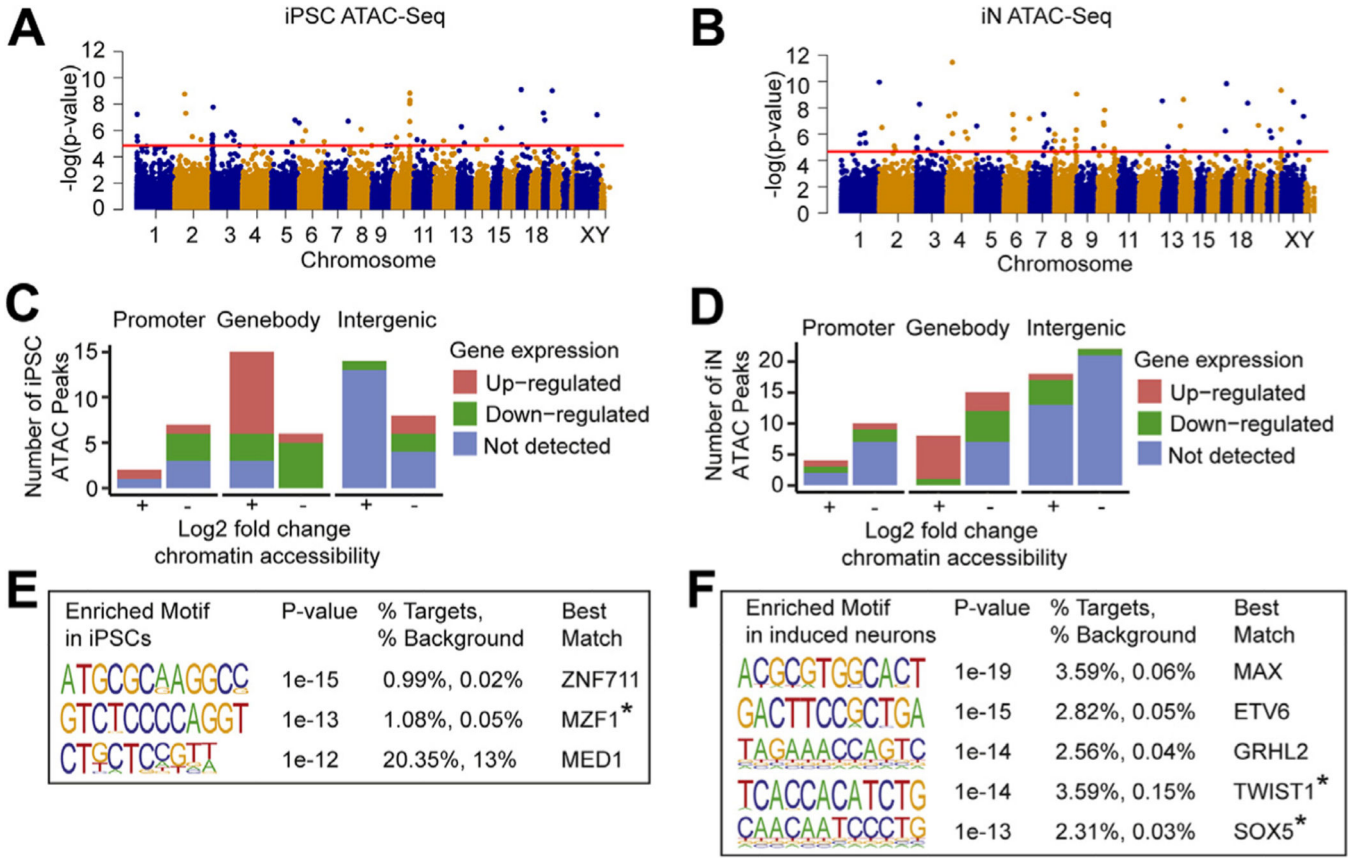

Figure 4.

ATAC-Seq shows altered chromatin accessibility in 15q13.3 microdeletion lines. (**A**, **B**) Genome-wide distribution of peaks identified from ATAC-Seq in iPSCs (**A**) and iNs (**B**). Peaks above red threshold line have adjusted p # .05. (**C**, **D**) Differentially accessible ATAC-Seq peaks in iPSCs and iNs, split by peak location, direction of chromatin accessibility change, and direction of expression change in nearest gene. (**E**, **F**) Enriched motifs in iPSCs and iNs from de novo Homer analysis with p value ≤ 10^{-12}, best match TF expressed in the same tissue, and best match score ≥ 0.6. *Gene has known association with Wnt signaling pathway. ATAC-Seq, assay for transposase-accessible chromatin sequencing; iN, induced neuron; iPSC, induced pluripotent stem cell; TF, transcription factor.

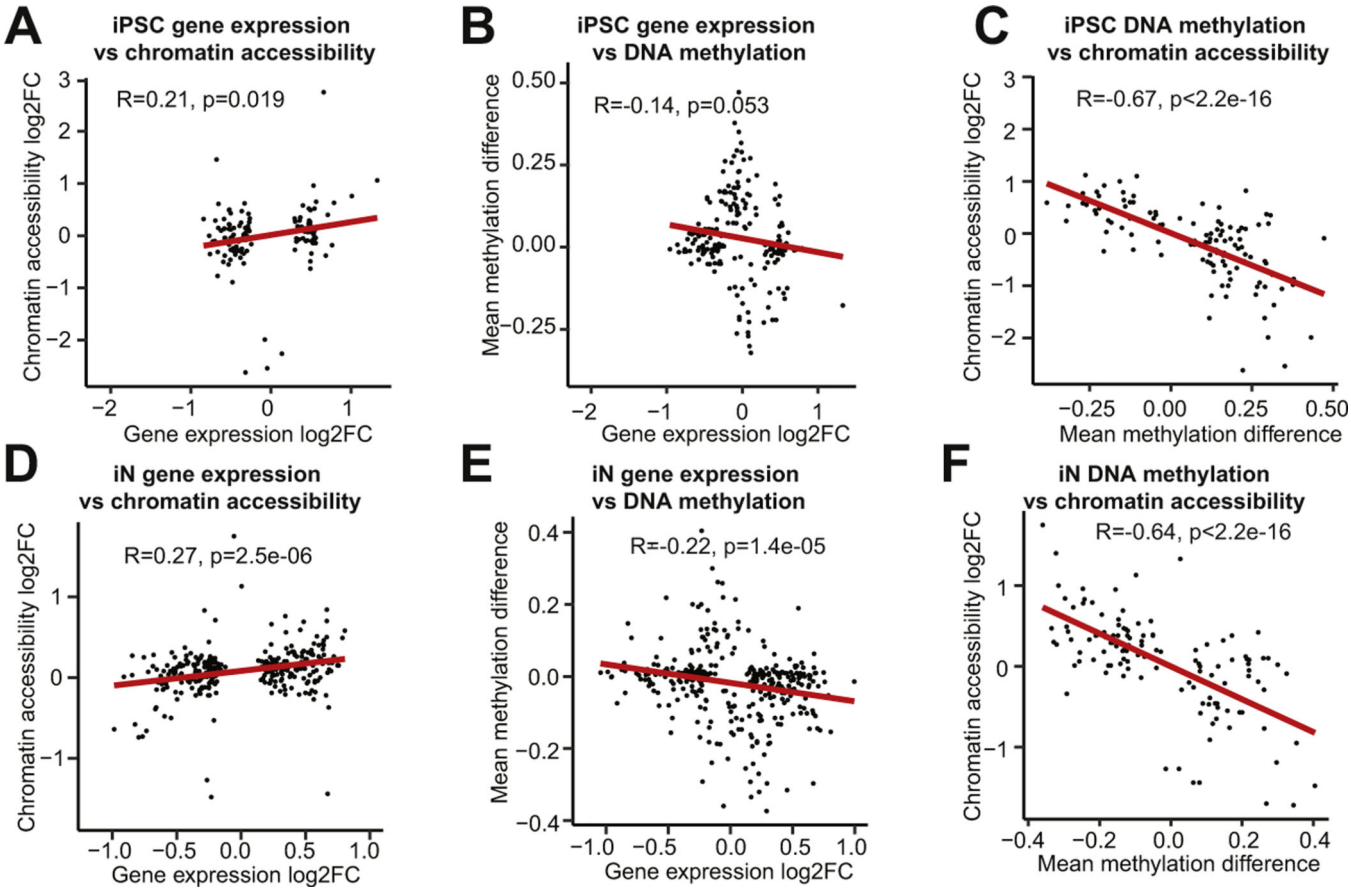

Figure 5.

Multiomics correlation analysis. Correlations between gene expression log2 FC and chromatin accessibility log2 FC (**A**, **D**), between gene expression log2 FC and mean DNA methylation difference (**B**, **E**), and between mean DNA methylation difference and chromatin accessibility log2 FC (**C**, **F**) are shown. FC, fold change; iN, induced neuron; iPSC, induced pluripotent stem cell;

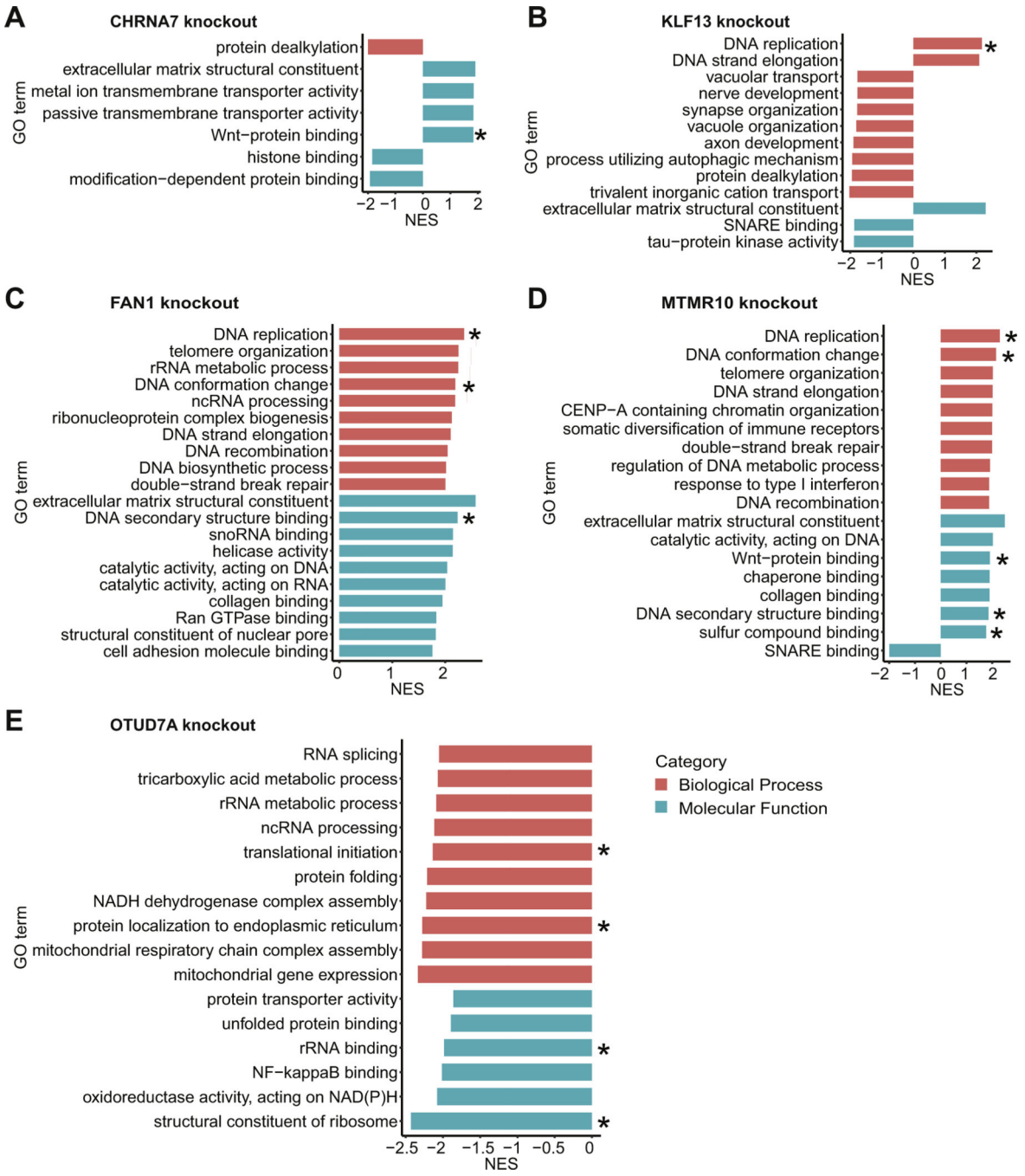

Figure 6.

CRISPR–Cas9 knockout RNA-Seq analysis. Significant GO terms from gene set enrichment analysis of RNA-Seq datasets for knockouts of *CHRNA7* (**A**), *KLF13* (**B**), *FAN1* (**C**), *MTMR10* (**D**), and *OTUD7A* (**E**) are shown. The top 10 terms in each category based on FDR are listed, ordered by NES. *GO term also enriched in 15q13.3 microdeletion induced neurons. CRISPR, clustered regularly interspaced short palindromic repeats; FDR, false discovery rate; GO, Gene Ontology; ncRNA, noncoding RNA; NES, normalized enrichment

score; NF, nuclear factor; RNA-Seq, RNA sequencing; rRNA, ribosomal RNA; snoRNA, small nucleolar RNA.

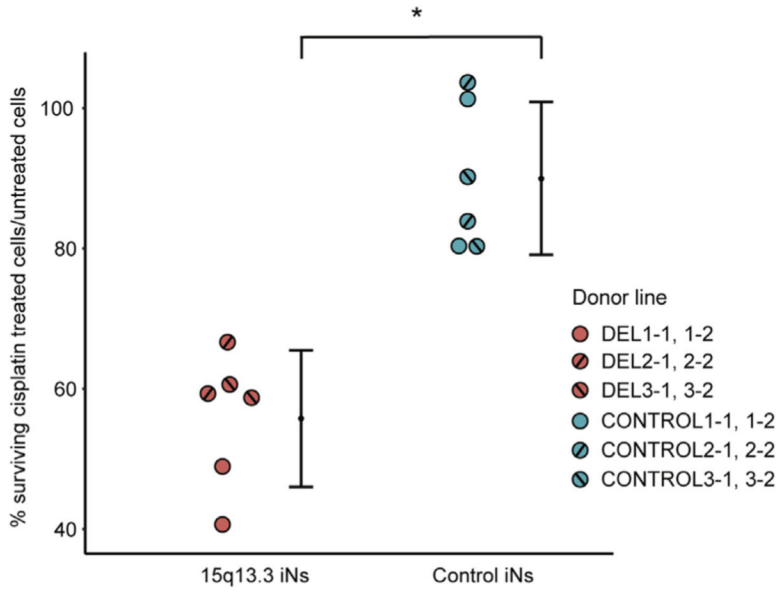

Figure 7.

Cell survival after cisplatin exposure as a measure of altered DNA damage response in 15q13.3 microdeletion iNs. Mean percentages (with 95% confidence intervals) of surviving cisplatin-treated cells normalized to untreated cells in 15q13.3 microdeletion iNs and control iNs are shown. *p <.005 by nested *t* test. iN, induced neuron.

Biol Psychiatry. Author manuscript; available in PMC 2022 August 08.

KEY RESOURCES TABLE

Resource Type	Specific Reagent or Resource	Source or Reference	Identifiers	Additional Information
Add additional rows as needed for each resource type	**Include species and sex when applicable.**	**Include name of manufacturer, company, repository, individual, or research lab. Include PMID or DOI for references; use "this paper" if new.**	**Include catalog numbers, stock numbers, database IDs or accession numbers, and/or RRIDs. RRIDs are highly encouraged; search for RRIDs at https://scicrunch.org/resources.**	**Include any additional information or notes if necessary.**
Antibody	mouse monoclonal SSEA4	ESI Bio	ST11015	
Antibody	mouse monoclonal TRA-1–60	ESI Bio	ST11016	
Antibody	rabbit polyclonal Nanog	Stemgent	09–0020	
Antibody	rabbit monoclonal TUJ1	Biolegend	1–15-56	
Antibody	rabbit polyclonal VGLUT1	Synaptic Systems	135 302	
Antibody	mouse monoclonal MAP2	Sigma Aldrich	M1406	
Antibody	Alexa Fluor 488 goat anti-mouse	Life Technologies	A11029	
Antibody	Alexa Fluor 555 goat anti-mouse	Life Technologies	A21422	
Antibody	Alexa Fluor 555 goat anti-rabbit	Life Technologies	A21428	
Chemical Compound or Drug	CIS-PLATINUM(II)DIAMMINE DICHLORIDE	Sigma Aldrich	P4394	
Sequence-Based Reagent	CRISPR PCR validation primers, Supplementary Table S3	This paper	N/A	
Sequence-Based Reagent	CRISPR gRNAs, Supplementary Table S3	This paper	N/A	
Software; Algorithm	BEDTools	PMID: 20110278	RRID:SCR_006646	
Software; Algorithm	BWA	PMID: 19451168, PMID: 20080505	RRID:SCR_010910	
Software; Algorithm	CNVnator	PMID: 21324876	RRID:SCR_010821	
Software; Algorithm	Tophat	PMID: 19289445	RRID:SCR_013035	
Software; Algorithm	DESeq2	PMID: 25516281	RRID:SCR_015687	
Software; Algorithm	WebGestalt	PMID: 24233776, PMID:15980575, PMID:14975175	RRID:SCR_006786	
Software; Algorithm	variancePartition	PMID: 27884101		
Software; Algorithm	CIBERSORT	PMID:25822800	RRID:SCR_016955	
Software; Algorithm	Bowtie	PMID:22388286, PMID:19261174	RRID:SCR_005476	
Software; Algorithm	Bismark	PMID: 21493656	RRID:SCR_005604	
Software; Algorithm	methylKit	PMID: 23034086	RRID:SCR_005177	

Resource Type	Specific Reagent or Resource	Source or Reference	Identifiers	Additional Information
Add additional rows as needed for each resource type	**Include species and sex when applicable.**	**Include name of manufacturer, company, repository, individual, or research lab. Include PMID or DOI for references; use “this paper” if new.**	**Include catalog numbers, stock numbers, database IDs or accession numbers, and/or RRIDs. RRIDs are highly encouraged; search for RRIDs at https://scicrunch.org/resources.**	**Include any additional information or notes if necessary.**
Software; Algorithm	metilene	PMID: 26631489		
Software; Algorithm	MACS	PMID: 18798982	RRID:SCR_013291	
Software; Algorithm	HOMER	PMID:20513432	RRID:SCR_010881	
Software; Algorithm	DiffBind		RRID:SCR_012918	
Software; Algorithm	Graphpad Prism		RRID:SCR_002798	
Commercial Assay Or Kit	CytoTune-iPS 2.0 Sendai Reprogramming Kit	Life Technologies	A16517	
Commercial Assay Or Kit	Direct-zol RNA MiniPrep Kit	Zymo Research	R2051	
Commercial Assay Or Kit	NEBNext Ultra Directional RNA Library Prep Kit	New England Biolabs	E7420S	
Commercial Assay Or Kit	Quick-DNA Universal Kit	Zymo Research	D4068	
Commercial Assay Or Kit	TruSeq DNA Nano Library kit	Illumina	20015965	
Commercial Assay Or Kit	Dynabeads mRNA Purification Kit	Thermo Fisher Scientific	61006	
Commercial Assay Or Kit	KAPA Library Prep Kit	Roche	KK8232	
Commercial Assay Or Kit	Qiagen MinElute Kit	Qiagen	28004	
Cell Line	iPSC cell lines, Supplementary Tables S1, S2	This paper	N/A	
Deposited Data; Public Database	GSE135131	NCBI GEO DataSets	RRID:SCR_005012	
Deposited Data; Public Database	SRA PRJNA557485	NCBI Sequence Read Archive	RRID:SCR_004891	